Estimation of Surface Characteristics Using GNSS LH-Reflected Signals: Land Versus Water

Estimation of Surface Characteristics Using GNSS LH-Reflected Signals: Land Versus Water

Yan Jia, Patrizia Savi, *Senior Member, IEEE*, Davide Canone, and Riccardo Notarpietro

***Abstract*—Estimating the characteristics of soil surface represents a significant area in applications such as hydrology, climatology, and agriculture. Signals transmitted from Global Navigation Satellite Systems (GNSSs) can be used for soil monitoring after reflection from the Earth's surface. In this paper, the feasibility of obtaining surface characteristics from the power ratio of left-hand (LH) reflected signal-to-noise ratio (SNR) over direct right-hand (RH) is investigated. The analysis was done regardless of the surface roughness and the incoherent components of the reflected power. First, the analysis was carried out on data collected during several *in situ* measurements in controlled environments with known characteristics. Then, further data were collected by a GNSS receiver prototype installed on a small aircraft and analyzed. This system was calibrated on the basis of signals reflected from water. The reflectivity and the estimated permittivity showed good correlation with the types of underlying terrain.**

***Index Terms*—Global Navigation Satellite System (GNSS) reflectometry, permittivity retrieval, signal-to-noise ratio (SNR).**

I. Introduction

OVER the last two decades, Global Navigation Satellite System-Reflectometry (GNSS-R), has gained increasing interest among the scientific community thanks to the development of positioning systems. In this technique, the GPS signals reflected from the ground are measured using a ground-based or aircraft-based passive receiver [1]. Sea-state retrieval, sea ice and snow characterization and soil moisture retrieval are among the various applications implementing the GNSS-R technique (see e.g. [2]–[3]). Recently, several ground based field experiments and some airborne campaigns have shown the feasibility of retrieving soil moisture using reflected GNSS signals [4]–[13]. To this end, a different method has been proposed to analyze the phase and magnitude of the signal-to-noise ratio (SNR) modulation pattern arising from the interference of the direct and reflected signals. In this model the soil is considered as a stratified medium with a complex dielectric permittivity given by well-known mixing models [4], [5]. The interference pattern technique (IPT) is based on the measurement of power fluctuations of the vertical polarized signal given by the interference of the direct and reflected GNSS signals [6]–[8]. The bistatic method is based on the measurement of direct and reflected signals and the evaluation of the SNR [9], [10].

In this work, *in situ* GNSS-R campaigns in two well-known environments are described. The first experimental field is located in Grugliasco, Torino, Italy [11]. The soil is 70% sand [12], and it is covered by nonirrigated permanent meadows. The second area is located in Agliano, Asti, Italy, and it has a soil composition with 52% silt and 37% clay. The dielectric constant was evaluated from the LH reflected signal coming from satellites with a high elevation angle and the results compared with local measurements based on time-domain reflectometry (TDR).

The data collected by a GNSS receiver prototype were also analyzed. This prototype was developed by Istituto Superiore Mario Boella (ISMB) in the framework of the Italian project SMAT-F2 (System of Advanced monitoring of the Territory – phase 2). It can be easily installed on small aircraft due to its light weight and small size. During the December 11, 2014, measurements, the aircraft flew over the area around the Avigliana Lakes, Torino, Italy. Both direct and reflected GPS signals were measured using a right-hand circular-polarized (RHCP) and a left-hand circular-polarized (LHCP) antenna, respectively.

The power ratio of LHCP-reflected SNR over direct RHCP SNR was evaluated, regardless of the surface roughness and incoherent components. The reflected signal was processed with an open-loop approach, in order to obtain delay Doppler maps (DDMs) and the corresponding delay waveforms. SNRs time series were estimated from several noncoherently integrated delay waveforms. A calibration process was performed using the signals reflected from the lakes. The reflectivity obtained from different satellites was related to the type of terrain.

II. Retrieval Process from LHCP Reflected Signals

In this section, the retrieval of the dielectric constant assuming a perfectly smooth surface (specular reflection) is described (see Fig. 1). In this case, the reflected GPS signals are predominately LHCP [13], [14], especially for satellites with high elevation (angles greater than 60°).

The total electromagnetic field received by the down-looking antenna is the sum of various contributions scattered from the Earth's surface. Two kinds of contributions can be defined: coherent and incoherent. In the coherent part, the phase distribution is constant, while in the incoherent part the phase is random and uniformly distributed over an interval of 2π. In [15] it is shown

Manuscript received September 16, 2015; revised March 24, 2016 and June 01, 2016; accepted June 10, 2016. This work was supported in part by the SMAT-F2 project of Regione Piemonte.

Y. Jia and P. Savi are with the Electronic and Telecommunication Department, Politecnico di Torino, Torino 10129, Italy (e-mail: yan.jia@polito.it; patrizia.savi@polito.it).

D. Canone is with the Dipartimento Inter-ateneo di Scienze Progetto e Politiche del Territorio (DIST), Politecnico e Università di Torino, Torino 10125, Italy (e-mail: davide.canone@unito.it).

R. Notarpietro was with the Electronic and Telecommunication Department, Politecnico di Torino, Torino 10129 Italy. He is now with the EUMETSAT, Darmstadt 64295, Germany (e-mail: riccardo.notarpietro@eumetsat.int).

Color versions of one or more of the figures in this paper are available online at http://ieeexplore.ieee.org.

Digital Object Identifier 10.1109/JSTARS.2016.2584092

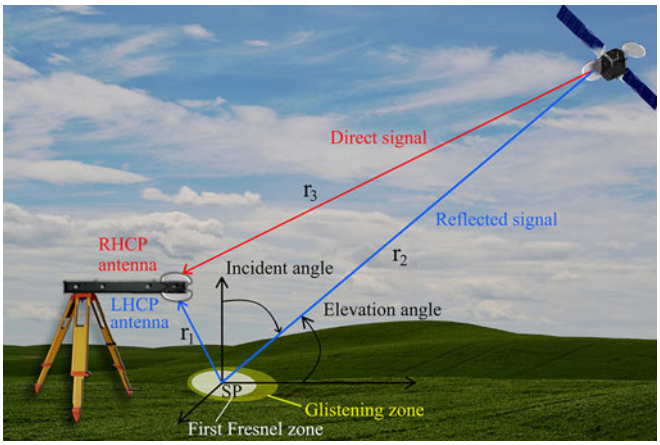

Fig. 1. Bistatic radar geometry.

that, for a smooth surface the coherent contribution is mainly LH polarized.

L-band signals are not impacted by atmospheric attenuation and normally have a good penetration through vegetation [15]. If the surface can be considered smooth, the noncoherent component assumes very low values that can be ignored and the total power received by the antenna can be approximated with the coherent part only [13].

The retrieval process aims to establish the link between received LHCP reflected signals and the dielectric constant of the soil. From the dielectric constant, if the characteristics of the soil are known, the soil moisture can be obtained by applying several well-established models (see, for example, the empirical model given in [16] and [17]). These models may be useful for the monitoring of a field of known characteristics in terms of sand, clay percentage, etc. In a general case, more powerful techniques of inverse scattering should be used.

The bistatic radar equation describes the coherent component in the GPS bistatic radar. Subscript lr represents the scattering when a satellite incident signal (RH polarized) is scattered by the surface and inverts the polarization to the LH [15]:

$$P_{\mathrm{lr}}^{\mathrm{coh}} = R_{\mathrm{lr}} \frac{P_t G_t G_r \lambda^2}{(4\pi)^2 (r_1 + r_2)^2} \tag{1}$$

where P_t is the transmitted signal power, G_t is the transmitter antenna gain, G_r is the receiver antenna gain and λ is the wavelength ($\lambda = 19.042$ cm for GPS L1 signal), r_1 is the distance between the receiver and the specular point, r_2 between the specular point and the satellite, and R_{lr} is the power reflectivity, which depends on the surface roughness as [18]

$$R_{\mathrm{lr}}(\theta) = |\Gamma_{\mathrm{lr}}(\theta)|^2 \chi(z) \tag{2}$$

where Γ_{lr} is the Fresnel reflection coefficient and $\chi(z)$ is the probability density function of the surface height z. Under the assumption of a perfectly flat surface $\chi(z) = 1$.

Combining (1) and (2), the processed SNR of peak power can be written as

$$\mathrm{SNR}_{\mathrm{peak}}^{\mathrm{refl}} = \frac{P_{\mathrm{lr}}^{\mathrm{coh}} G_D}{P_N} = \frac{P_t G_t G_r \lambda^2 G_D}{(4\pi)^2 (r_1 + r_2)^2 P_N} |\Gamma_{\mathrm{lr}}|^2 \tag{3}$$

where P_N is the noise power and G_D is the processing gain due to the de-spread of the GPS C/A code. The SNR peak power of the direct RHCP signal is

$$\mathrm{SNR}_{\mathrm{p}}^{\mathrm{d}} = \frac{P_t G_t G_r \lambda^2 G_D}{(4\pi)^2 r_3^2 P_N} \tag{4}$$

where r_3 is the distance between the transmitter and receiver. It has to be noted that the receiver gain G_r and noise power P_N of the direct signal (4) are not equal to those in (3) for the reflected signal. Therefore, a calibration process is needed. The ratio of the reflected SNR (3) over the direct SNR (4) is given by

$$\frac{\mathrm{SNR}_{\mathrm{peak}}^{\mathrm{reflect}}}{\mathrm{SNR}_{\mathrm{peak}}^{\mathrm{direct}}} = \frac{r_3^2}{(r_1 + r_2)^2} |\Gamma_{\mathrm{lr}}|^2 \, C \tag{5}$$

where C is a calibration parameter summarizing the uncertainties of G_r and P_N.

The reflection coefficient Γ_{lr} can be written as a linear combination of vertical and horizontal polarization [19]

$$\Gamma_{\mathrm{lr}} = \frac{1}{2} (\Gamma_{\mathrm{vv}} - \Gamma_{\mathrm{hh}}) \tag{6}$$

where Γ_{vv} and Γ_{hh} are the Fresnel coefficients for horizontal and vertical polarization [20]

$$\begin{aligned} \Gamma_{\mathrm{hh}}(\theta) &= \frac{\cos\theta - \sqrt{\varepsilon_r - \sin^2\theta}}{\cos\theta + \sqrt{\varepsilon_r - \sin^2\theta}} \\ \Gamma_{\mathrm{vv}}(\theta) &= \frac{\varepsilon_r \cos\theta - \sqrt{\varepsilon_r - \sin^2\theta}}{\varepsilon_r \cos\theta + \sqrt{\varepsilon_r - \sin^2\theta}} \end{aligned} \tag{7}$$

where θ is the incident angle, $\varepsilon_r = \varepsilon_{r2}/\varepsilon_{r1}$ in which ε_{r2} is the complex permittivity of the soil and ε_{r1} is the complex permittivity of the air. For the soil (dry and wet) the imaginary part of the permittivity can be neglected [21], [22]. With this hypothesis, the real part of the permittivity can be obtained from (3) together with (6), when only the LH reflected signal is known. If the LH reflected signal is normalized to the direct signal, the real permittivity can be obtained from (5) with water calibration. For satellites with high elevation angles $|\Gamma_{\mathrm{vv}}| = |\Gamma_{\mathrm{hh}}|$, the real part of the permittivity can be obtained by solving the equation for Γ_{vv} [23], or for Γ_{hh} as in [22] and [24].

III. Static Measurements

Several static measurements were carried out in two different sites. The first site is a controlled environment located in Grugliasco, Torino (45°03'58.5"N, 7°35'33.8"E), in the Dipartimento Inter-ateneo di Scienze Progetto e Politiche del Territorio (DIST). In this place, a wide field of known characteristics (mainly 50% sand) was available. The second site located in Agliano (44° 47'29.1"N, 8° 15'19.8"E) is an area of smooth hills mainly devoted to wine production. In this second case, the composition of the soil is 50% silt and 37% clay.

GNSS-R equipment and TDR setup were used to make measurements before and after rain in bare fields, which were intentionally chosen due to their different terrain composition. Data obtained with GNSS-R measurements are related to TDR

TABLE I
COMPOSITION OF THE SOIL FOR THE GRUGLIASCO EXPERIMENT

Coarse Sand(%)	Fine Sand(%)	Very Fine Sand(%)	Coarse Silt(%)	Fine Silt(%)	Clay(%)	Organic Matter(%)
15.5	50.1	16.1	5.3	8.2	4.8	1.4

TABLE II
COMPOSITION OF THE SOIL FOR THE AGLIANO EXPERIMENT

Coarse Sand(%)	Fine Sand(%)	Coarse Silt(%)	Fine Silt(%)	Clay(%)	Organic Matter(%)
1.1	10.5	6.4	44.5	36.8	0.7

Fig. 2. Static measurement setup in grugliasco (left panel) and agliano (right panel).

measurements that can provide high resolution and reliable permittivity profiles [25]. In the following, four campaigns are discussed in details:

1) Grugliasco (dry condition), January 27, 2016
2) Agliano (dry condition), February 5, 2016
3) Grugliasco (wet condition), March 3, 2016
4) Agliano (wet condition), March 7, 2016.

In Tables I and II, the composition (volume percentage and type of sand, clay) of the soil for the two sites is reported. According to the United States Department of Agriculture (USDA) Classification System, the soil of the sites of Grugliasco and Agliano belong to the loamy sand and silty clay loam textural classes, respectively [26].

The GNSS-R system consists of two commercial front-ends connected to two antennas and PCs for data acquisition. The antennas and the front ends were mounted on a metal bar fixed on a tripod for a more efficient adjustment of the orientation of the antennas (see Fig. 2). The RHCP antenna was pointing upwards for the measurement of the direct signal, while the antenna with LH circular polarization was pointing downwards for the measurement of the reflected signal [27], [28].

The antennas used in the setup were active antennas produced by ANTCOM Corp. [29] and are able to receive a GPS signal in L1 band and L2 band with LH and RH polarizations. The receivers used were SiGe GN3S v2 USB RF front-end, developed by the Colorado Center For Astrodynamics Research [30]. The acquisition of GPS data received by the antennas were performed by using N-Grab GNSS data grabber developed by the NavSAS group [31]. The raw data collected by the N-Grab were post-processed for obtaining the SNR of each satellite.

The values of the permittivity obtained from the GNSS-R signals were compared with the results obtained from local measurements based on the time-domain reflectometry (TDR) technique [32]. The measurements were performed with a three-rod sensor (length 15 cm) and Tektronix Metallic Cable Tester 1502 manufactured by Tektronix Inc., Beaverton, OR, USA. The position of the TDR sensor was not perpendicular to the terrain but tilted to 30°. In this position, only around 7 cm of the surface were taken into account in the TDR measurements. This was done in order to compare the TDR results with those obtained with GNSS-R that sense only the first few centimeters of the surface. The major axis of the Fresnel zone (the region surrounding the specular point from which power is reflected with a phase change across the surface constrained to π radians, see Fig. 1) for satellites in our geometrical condition (high elevation angle and a height of tripod of 1.5 m) was around 1 m. The TDR portable system was then moved around to cover this area. An average value of permittivity and soil moisture were obtained.

A. Measurements in Grugliasco

The static measurement setup in Grugliasco is shown in Fig. 2 (left panel). The bar on which the antennas were mounted was kept horizontal at a height of 1.45 m.

Concerning the TDR measurement, the value of permittivity was obtained for each measurement from the travel time along the TDR probe and an average value of 6.4 in dry condition was calculated. By considering the average value of 7 for the permittivity and using the model reported in [25], a soil moisture of 10% can be estimated. The soil moisture calculated from the permittivity is very low because the measurement was performed after a long period of drought. The soil moisture calculated is close to the minimum observable value in the experimental field, and is consistent with the results of [11]. After a rainy period of one week the average measured value was 9 corresponding to a soil moisture of 16%.

In Table III, the average values of SNR were obtained on January 27 (dry condition) and March 3 (wet condition). The values of permittivity were obtained from (3) with considering the Γ_{vv} component. It was observed that the values with an elevation angle greater than 60° are close to those results obtained by TDR technique. For PRN 6 and PRN24 that have low elevation angles, the approximation of $|\Gamma_{\mathrm{vv}}| = |\Gamma_{\mathrm{hh}}|$ could not be applied. Moreover, the results of PRN13 are not very good. This is probably due to some interferences caused by the position of this satellite with respect to the receiving antenna.

B. Measurements in Agliano

The same measurements were carried out in Agliano (see Fig. 2 right panel). In Table IV, the average values of SNR

TABLE III
RESULTS FOR GRUGLIASCO: DRY CONDITION AND WET CONDITION

Meas.	PRN 23			PRN 9			PRN 6		
	Ele (deg)	SNR(dB)	Eps	Ele (deg)	SNR(dB)	Eps	Ele (deg)	SNR(dB)	Eps
1 dry	77.7	5	6	63.2	3	5	50.5	−5	2
2 dry	70.9	4	6	70	3	5	55.2	1	4
	PRN15			PRN13			PRN24		
	Ele (deg)	SNR(dB)	Eps	Ele (deg)	SNR(dB)	Eps	Ele (deg)	SNR(dB)	Eps
1 wet	72	10	8	59.7	6	4	43.8	0.5	3
2 wet	72.2	11	9	58.7	4	3	44.2	−3	2

TABLE IV
RESULTS FOR AGLIANO: DRY CONDITION AND WET CONDITION

Meas.	PRN 13			PRN 28			PRN 15		
	Ele (deg)	SNR(dB)	Eps	Ele (deg)	SNR(dB)	Eps	Ele (deg)	SNR(dB)	Eps
1 dry	79.6	12	18	52.6	7	6	57.5	11	16
2 dry	73.7	13	15	63	11	14	48.1	7	10
	PRN 30			PRN7			PRN5		
	Ele (deg)	SNR(dB)	Eps	Ele (deg)	SNR(dB)	Eps	Ele (deg)	SNR(dB)	Eps
1 wet	72.5	13	24	67.8	9	20	49.1	6	11
2 wet	83	14	22	57.1	8	19	50.1	6	10

obtained on February 5 (dry condition) and March 7 (wet condition) are shown. In this case, the average relative permittivity measured by TDR in dry condition was 15. After a rainy period of one week, the average measured value was 22. These values of permittivity correspond to a soil moisture of 28% and 36%, respectively. As in the previous case, the values of permittivity obtained by the GNSS-R measurements are close to those of TDR results only for satellites with high elevation angles.

IV. ON-BOARD MEASUREMENTS

A. GNSS Receiver Prototype

A GNSS receiver prototype was developed by Istituto Superiore Mario Boella (ISMB) [33] in the framework of the Italian project SMAT-F2 (System of Advanced monitoring of the Territory – phase 2). The hardware architecture consists of two double-chain radio frequency front-ends and a microprocessor board. The front-end receivers produced by NSL Stereo [34] are connected to a microprocessor board developed based on the Open-Android (ODROID)-X2 platform [35]. The system is mounted in a carbon fiber box, specifically designed with a wing profile for aerodynamic requirements. The prototype dimensions are 75 mm $\times$ 150 mm $\times$ 250 mm and its weight is less than 3 kg making it sufficiently light and compact to be mounted on board small aircrafts or UAV. Two antennas were connected to the front-ends. One was a conventional GNSS L1 patch, up-looking RHCP antenna, to receive the direct signal from satellites. The other down-looking antenna (LH polarized antenna of Antcom [29]) measured the signals after reflection from the ground.

Fig. 3. GNSS-R prototype mounted on digisky P92 aircraft.

The raw data were stored on board in order to be post-processed [31]. Due to the large amount of memory (GB/min) required for storing the raw data, the duration of the data collection was limited. The post-processing was made with the software SOPRANO [36]. A coherent and noncoherent integration time technique was adopted during the post-processing in order to mitigate the noise. Due to the characteristics of the reflected surface, the reflected signal is much weaker than the direct one and it is not continuous in time. Hence, in order to detect the reflected signal, a channel aiding was implemented by using the direct signal information. During data processing of reflected signals, a range of expected delays was defined depending on the direct signal delays and system geometry. The reflected peak value should appear in the range of the delays. However, when this did not occur, we adjusted the noncoherent time to repeat the search.

The optimal coherent and noncoherent time interval depends on the coherence time of the scattered signal. In GPS-reflectometry applications, a coherent time of 1 ms, combined with a number of noncoherent sums in the order of 100–1000 are generally used [27], [28]. However, for the typical altitude of the flight analyzed in this work, the expected coherence time was 0.1−0.5 s.

B. Results

The GNSS receiver prototype was mounted on a Digisky P92 aircraft (see Fig. 3) and the aircraft flew over the area around the Avigliana lakes during the measurements of December 11, 2014. The vegetation was ignored since the estimation of the quantitative impact is very difficult, being a combination of incidence angle, wavelength, biomass volume, height, and loss component induced by the dielectric constant of water-containing stalks and leaves. And it is often modeled separately from the bare soil surface as a signal attenuation proportional to vegetation water content [15].

In Fig. 4, the sky-plot of GPS satellites at the 1570th second of the flight is shown.

In the first flight route (see Fig. 5), PRN4 (elevation 78°) and PRN32 (elevation 87°) were considered because the specular points corresponding to these satellites fell on the lakes' surfaces and it was possible to calibrate the system.

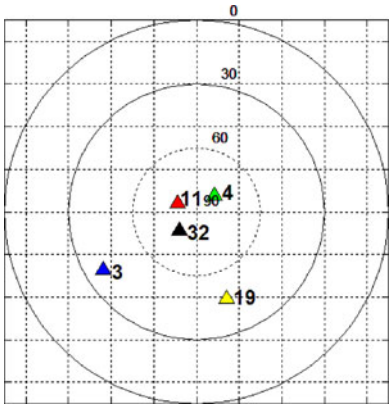

Fig. 4. Skyplot December 11 flights.

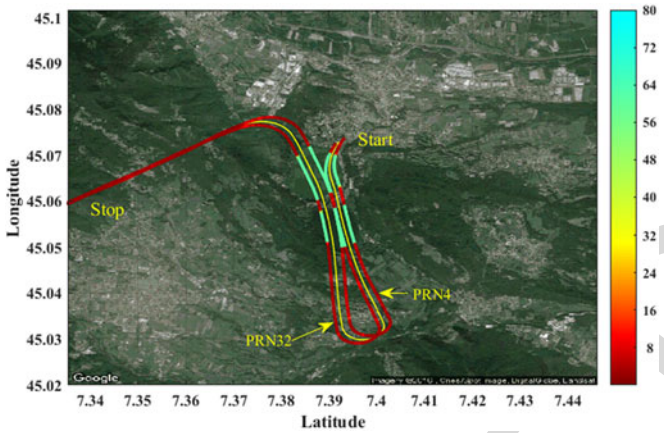

Fig. 5. Route flight (yellow line), specular reflection points of PRN4 and PRN32 with the levels of dielectric constant values.

The reflected signals were postprocessed with an open-loop approach, in order to obtain delay Doppler maps (DDMs) and the corresponding delay waveforms. SNRs time series were estimated from noncoherently integrated delay waveforms. Both direct and reflected signals were processed to obtain the SNR and a calibration process was performed through the over-water condition to determine the calibration constant C of (5).

In Figs. 6 and 7, the normalized power reflectivity of LH reflected signal normalized to RH direct signal are shown. The high reflectivity values correspond to the return flight over the two lakes. The values of the real part of permittivity were obtained from (5) and (6). They are superimposed on google map as shown in Fig. 5. On the lakes, the value of permittivity is around 80, whereas on the land is from 4 to 30.

In the second flight route (see Fig. 8), PRN 3 (elevation 38.2°), 11 (elevation 80.3°), and 19 (elevation 46.7°) are also taken into account. In this case only the PRN11 has a great elevation angle. The reflection points for these satellites are also shown in Fig. 8. The normalized reflectivity is shown in Fig. 9. High values of reflectivity correspond to the presence of the almost specular reflecting surface of the lake. This is confirmed also for low elevation satellites such as PRN19 and PRN3.

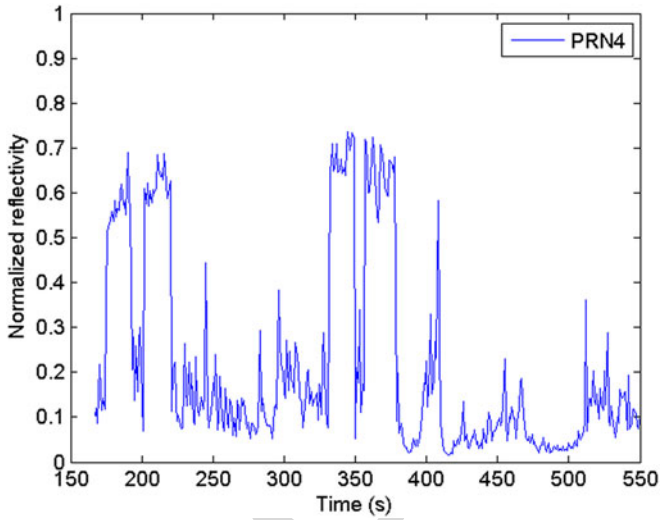

Fig. 6. Normalized power reflectivity of PRN4.

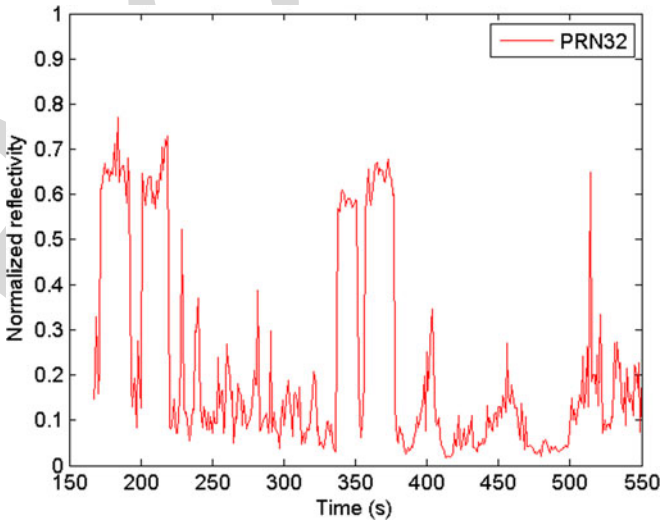

Fig. 7. Normalized power reflectivity of PRN32.

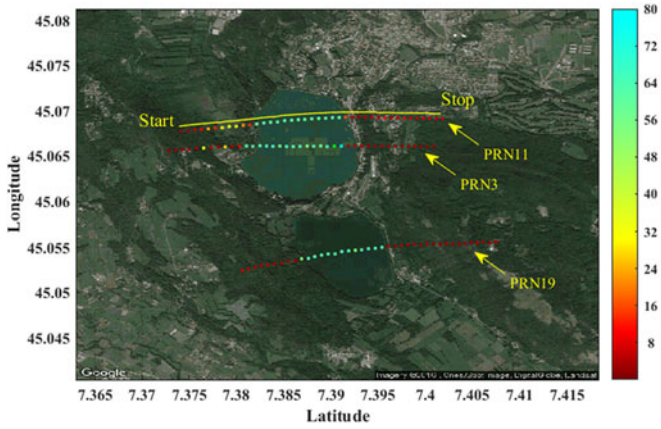

Fig. 8. Route flight (yellow line), specular reflection points of PRN3, PRN11, and PRN19 with the levels of dielectric constant values.

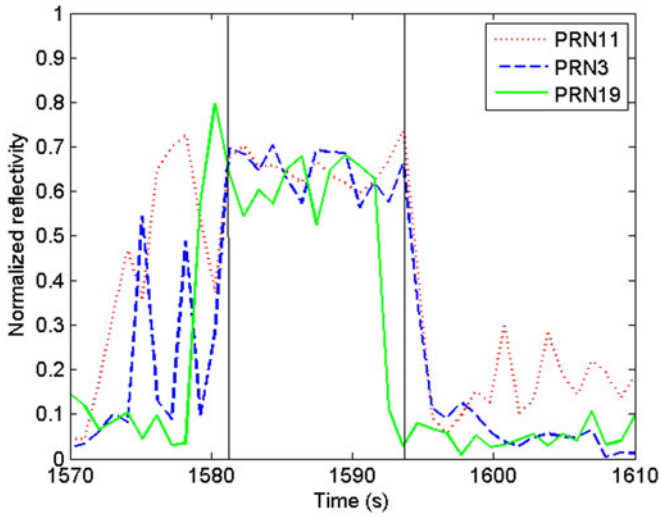

Fig. 9. Normalized power reflectivity of PRN11, PRN3, and PRN19.

In Fig. 8, the values of the real part of the permittivity are also shown and are in good agreement with the land and water condition.

V. Conclusion

The use of GNSS-R reflected signals to monitor the Earth's surface was analyzed with *in situ* and on-board measurements. The values of the dielectric constant obtained with *in situ* GNSS-R measurements were compared with TDR results for validating the retrieval process. Data collected during a flight over the Avigliana lakes by a GNSS receiver prototype developed by the Istituto Superiore Mario Boella (ISMB) were post-processed with an open-loop approach, Delay Doppler Maps and delay waveforms were obtained. The power reflectivity evaluated as the ratio of LH reflected signal to the direct RH signal and the estimated real permittivity showed good correlation with the types of underlying terrain.

Acknowledgment

The authors would like to thank the Istituto Superiore Mario Boella (ISMB) for the realization of the prototype, Digisky s.r.l. (Turin, Italy) for the flight campaigns performed with the Tecnam P92 aicraft and the Istituto per le Piante da Legno e Ambiente - I.P.L.A. S.p.A. for the individuation of the site for the static campaign.

References

[1] S. Jin, E. Cardellach, and F. Xie, *GNSS Remote Sensing: Theory, Methods and Applications*. New York NY, U.S.A.: Springer, 2014.

[2] C. Li, W. Huang, and S. Gleason, "Dual antenna-space based GNSS-R ocean surface mapping: Oil slick and tropycal cyclone sensing," *IEEE J. Sel. Top. Appl. Earth Obs. Remote Sens.*, vol. 8, no. 1, pp. 425–435, Jan. 2015.

[3] A. Alonso-Arroyo, A. Camps, H. Park, D. Pasqual, R. Onrubia, and F. Martin, "Retrieval of significant wave height and mean sea surface level using the GNSS-R interference pattern technique: Results from a three-month field campaign," *IEEE Trans. Geosci. Remote Sens.*, vol. 53, no. 6, pp. 3198–3209, Jun. 2015.

[4] V. U. Zavorotny, K. M. Larson, J. J. Braun, E. E. Small, E. D. Gutmann, and A. L. Bilich, "A physical model for GPS multipath caused by land reflections: Towards bare soil moisture retrieval," *IEEE J. Sel. Top. Appl. Earth Obs. Remote Sens.*, vol. 3, no. , pp. 100–110, Mar. 2010.

[5] K. M. Larson, J. J. Braun, E. E. Small, V. U. Zavorotny, E. D. Gutmann, and A. L. Bilich, "GPS multipath and its relation to near- surface soil moisture content," *IEEE J. Sel. Top. Appl. Earth Obs. Remote Sens.*, vol. 3, no. 1, pp. 91–99, Mar. 2010.

[6] N. Rodriguez-Alvarez, X. Bosch-Luis, A. Camps, *et al.*, "Soil moisture retrieval using GNSS-R techniques: Experimental results over a bare soil field," *IEEE Trans. Geosci. Remote Sens.*, vol. 47, no. 11, pp. 3616–3624, Nov. 2009.

[7] V. L. Mironov, S. V. Fomin, V. M. Konstantin, V. S. Anatoliy, and M. I. Mikhaylov, "The use of navigation satellites signals for determination the characteristics of the soil and forest canopy," in *Proc. IEEE Int. Symp. Geoscie. Remote Sens., Munich*, Germany, 2012, pp. 7527–7529.

[8] V. L. Mironov and K. V. Muzalevskiy, "The new algorithm for retrieval of soil moisture and surface roughness from GNSS reflectometry," *IEEE Int. Symp. Geosci. Remote Sens. Symp., Munich*, Germany, 2012, pp. 7530–7532.

[9] S. Katzberg, O. Torres, M. Grant, and D. Masters, "Utilizing calibrated GPS reflected signals to estimate soil reflectivity and dielectric constant: Results from SMEX02," *Remote Sens. Environ.*, pp. 17–28, 2005.

[10] A. Egido, M. Caparrini, G. Ruffini, S. Paloscia, E. Santi, L. Guerriero, N. Pierdicca, and N. Floury, "Global navigation satellite systems reflectometry as a remote sensing tool for agriculture," *Remote Sens.*, vol. 4, no. 8, pp. 2356–2372, 2012.

[11] M. Baudena, I. Bevilacqua, D. Canone, S. Ferraris, M. Previati, and A. Provenzale, "Soil water dynamics at a midlatitude test site: Field measurements and box modeling approaches," *J. Hydrol.*, vol. 414–415, pp. 329–340, 2012. [Online]. Available: http://dx.doi.org/10.1016/j.jhydrol.2011.11.009

[12] D. Canone, S. Ferraris, G. Sander, and R. Haverkamp, "Interpretation of water retention field measurements in relation to hysteresis phenomena," *Water Resour. Res.*, vol. 44, no. 4, pp. 1–14, 2008, W00D12. [Online]. Available: http://dx.doi.org/10.1029/2008WR007068

[13] D. Masters, A. Penina, and S. Katzberg, "Initial results of land-reflected GPS bistatic radar measurements in SMEX02," *Remote Sens. Environ.*, vol. 92, no. 4, pp. 507–520, 2004.

[14] F. Martín, F. M. Juan, A. Albert, V. l. Mercedes, C. Jordi, C. Adriano, M. Piles, L. Pipia, A. Tardà, and G. V. Alberto, "Airborne soil moisture determination using a data fusion approach at re[illegible] level," in *Proc. IEEE Int. Symp. Geosci. Remote Sens. Symp.*, 2011[illegible]3109–3112.

[15] R. D. De Roo and F. T. Ulaby, "Bistatic specular scattering from rough dielectric surfaces," *IEEE Trans. Antennas Propag.*, vol. 42, no. 2, pp. 220–231, Feb. 1994.

[16] M. C. Dobson, F. T. Ulaby, M. T. Hallikainen, and M. A. El-Rayes, "Microwave dielectric behaviour of wet soil—Part I: Empirical models and experimental observation," *IEEE Trans. Geoscie. Remote Sens.*, vol. 23, no. 1, pp. 25–34, Jan. 1985.

[17] J. Wang and T. Schmugge, "An empirical model for the complex dielectric permittivity of soils as a function of water content," *IEEE Trans. Geoscie. Remote Sens.*, vol. GE-18, no. 4, pp. 288–295, Oct. 1980.

[18] P. Beckmann and A. Spizzichino, *The Scattering of Electromagnetic Waves from Rough Surfaces*. Norwood, MA, USA: Artech House, 1963.

[19] W. L. Stutzman, *Polarization in Electromagnetic Systems*. Boston, USA: Artech House, 1993.

[20] R. Janaswamy, *Radiowave Propagation and Smart Antennas for Wireless Communications*. Norwell, MA, USA: Kluwer, 2001.

[21] J. Behari, Microwave Dielectric Behaviour of Wet Soils. Springer Science & Business Media. New York, USA., 2006.

[22] S. Hong and I. Shin, "A physically-based inversion algorithm for retrieving soil moisture in passive microwave remote sensing," *J. Hydrol.*, vol. 405, no. 1, pp. 24–30, 2011.

[23] A. Egido, G. Ruffini, M. Caparrini, C. Martín, E. Farrés, and X. Banqué, "Soil moisture monitorization using GNSS reflected signals," in *Proc. First Colloq. Sci. Fundam. Aspects Galileo Programme, Toulouse, France*, 2007, pp. 1–4.

[24] T. J. Jackson, R. Hurkmans, A. Hsu, and M. H. Cosh, "Soil moisture algorithm validation using data from the Advanced Microwave Scanning Radiometer (AMSR-E) in Mongolia," *Italian J. Remote Sens.*, vol. 30/31, pp. 39–52, 2004.

[25] G. C. Topp, J. L. Davis, and A. P. Annan, "Electromagnetic determination of soil water content: Measurements in coaxial transmission lines," *Water Resour. Res.*, vol. 16, no. 3, pp. 574–582, 1980.

[26] Soil Survey Laboratory Staff, "*Soil survey laboratory methods manual." USDA-SCS U.S. Government Printing Office*, Washington, DC, USA, *Soil Survey Investigations Report no. 42, Version 2.0.,* 1992.
[27] Y. Pei, R. Notarpietro, P. Savi, and M. Pini, "A fully software GNSS-R receiver for soil dielectric constant monitoring," 15th *Int. Conf. Electromagnet. Advanc. App. (ICEAA13)*, Torino, Italy, Sep. 9–13, 2013.
[28] Y. Pei, R. Notarpietro, P. Savi, and F. Dovis, "A fully software GNSS-R receiver for soil monitoring," *Int. J. Remote Sens.*, vol. 35, no. 6, pp. 2378–2391, 2014.
[29] Dual Polarization ANTCOM Antennas Catalog. Antcom Corp., Torrance, CA, USA. [Online] http://www.antcom.com/documents/catalogs/RHCP-LHCP-V-H-L1L2GPSAntennas.pdf (accessed on 30 June 2016).
[30] Colorado Center for Astrodynamics Research. Denver, CO, USA. [Online]. http://ccar.colorado.edu/gnss/ (accessed on 30 June 2016).
[31] Navigation Satellite System Group, Politecnico di Torino, Torino, TO, Italy. [Online]. http://www.det.polito.it/research/research_areas/telecommunications/navsas(accessed on 30 June 2016).
[32] P. Savi, I. A. Maio, and S. Ferraris, "The role of probe attenuation in the time-domain characterization of dielectrics," *Electromagnetics*, vol. 30, no. 6, pp. 554–564.
[33] Istituto Superiore Mario Boella (ISMB), Torino, Italy. [Online]. Available: http://www.ismb.it/
[34] NSL Stereo FE. [Online]. Available: http://www.nsl.eu.com/primo.html, accessed June 6, 2015.
[35] ODROID-X2 Platform. [Online]. Available: http://www.hardkernel.com/main/products/, accessed June 6, 2015.
[36] E. Falletti, D. Margaria, M. Nicola, G. Povero, and M. T. Gamba, "N-FUELS and SOPRANO: Educational tools for simulation, analysis and processing of satellite navigation signals," presented at the *IEEE Int. Conf. Frontiers Educ.*, Oklahoma City, USA, Oct. 23–26, 2013.

Yan Jia received the M.S. degree in telecommunications engineering from Politecnico di Torino, Turin, Italy, in 2013, where she is currently working toward the Ph.D. degree in electronics engineering.

Since 2013, she has been working in the Department of Electronics and Telecommunications, Politecnico di Torino, where she was involved in the GNSS-R antenna analysis. In 2014, she worked in the SMAT project, mainly focusing on the retrieval of soil moisture and biomass content. Her current research interests include Global Navigation Satellite System Reflectometry (GNSS-R) applications to land remote sensing and antenna design.

Patrizia Savi (SM'16) received the Laurea degree in electronic engineering from the Politecnico di Torino, Turin, Italy in 1985.

In 1986, she was a consultant in Alenia (Caselle Torinese, Italy) where she conducted research on the analysis and design of dielectric radomes. From 1987 to 1998, she was a Researcher with the Italian National Research Council. In 1998, she joined the Dipartimento di Elettronica, Politecnico di Torino, as an Associate Professor, where she is currently involved in teaching a course on electromagnetic field theory. Her current research interests include dielectric radomes, frequency-selective surfaces, waveguide discontinuities and microwave filters, high-altitude platform (HAP) propagation channels, Global Navigation Satellite System Reflectometry (GNSS-R) for soil moisture retrieval, microwave analysis, and characterization of carbon fiber and carbon nanotubes.

Davide Canone received the Graduate degree in forest and environmental sciences at the Agronomy Faculty of the University of Turin, Turin, Italy, in 2004, and the Ph.D. degree in agricultural, forest, and food sciences, curriculum agro-forest and agro-industrial economy and engineering from the University of Turin.

He collaborated with the Department of Agricultural, Forest, and Environmental Economics and Engineering (DEIAFA)—Division of Agricultural Hydraulics, University of Turin, from the year 2005. During the year 2007, he stayed six months at the Laboratory of Soil and Environmental Physics of the Federal Polytechnic of Lausanne, Switzerland, where he was involved in working on the characteristics of acoustic emissions during fluid front displacement in porous media. In August 2007, he was an Assistant Professor at the University of Turin. He is currently an Assistant Professor at the Interuniversity Department of Urban and Regional Studies and Planning of the Polytechnic and the University of Turin.

Riccardo Notarpietro received the Telecommun. Eng. Degree and the Ph.D. degree from Politecnico di Torino, Torino, Italy, in 1998 and in 2001, respectively, with a thesis on the subject of the atmosphere remote sensing exploiting GPS measurements from space and from ground.

He was an Assistant Professor in Electromagnetic Fields at Politecnico di Torino from 2006 to 2014. He was member of the Remote Sensing Group operating inside the Electronics Department. His main research areas were related to the retrieval of atmospheric profiles from GNSS Radio Occultation observations but also to the monitoring of soil properties using GNSS Reflectometry and to the tomographic reconstruction of 3-D water vapor fields using GNSS ground-based measurements. His fields of activities included also electromagnetic wave propagation and radarmeteorology. Since 2014 he is with EUMETSAT, Darmstadt, Germany, and providing support for the development of the new radio occultation mission on board the future European Polar System-Second Generation satellites.

Estimation of Surface Characteristics Using GNSS LH-Reflected Signals: Land Versus Water

Yan Jia, Patrizia Savi, *Senior Member, IEEE*, Davide Canone, and Riccardo Notarpietro

***Abstract*—Estimating the characteristics of soil surface represents a significant area in applications such as hydrology, climatology, and agriculture. Signals transmitted from Global Navigation Satellite Systems (GNSSs) can be used for soil monitoring after reflection from the Earth's surface. In this paper, the feasibility of obtaining surface characteristics from the power ratio of left-hand (LH) reflected signal-to-noise ratio (SNR) over direct right-hand (RH) is investigated. The analysis was done regardless of the surface roughness and the incoherent components of the reflected power. First, the analysis was carried out on data collected during several *in situ* measurements in controlled environments with known characteristics. Then, further data were collected by a GNSS receiver prototype installed on a small aircraft and analyzed. This system was calibrated on the basis of signals reflected from water. The reflectivity and the estimated permittivity showed good correlation with the types of underlying terrain.**

***Index Terms*—Global Navigation Satellite System (GNSS) reflectometry, permittivity retrieval, signal-to-noise ratio (SNR).**

I. Introduction

OVER the last two decades, Global Navigation Satellite System-Reflectometry (GNSS-R), has gained increasing interest among the scientific community thanks to the development of positioning systems. In this technique, the GPS signals reflected from the ground are measured using a ground-based or aircraft-based passive receiver [1]. Sea-state retrieval, sea ice and snow characterization and soil moisture retrieval are among the various applications implementing the GNSS-R technique (see e.g. [2]–[3]). Recently, several ground based field experiments and some airborne campaigns have shown the feasibility of retrieving soil moisture using reflected GNSS signals [4]–[13]. To this end, a different method has been proposed to analyze the phase and magnitude of the signal-to-noise ratio (SNR) modulation pattern arising from the interference of the direct and reflected signals. In this model the soil is considered as a stratified medium with a complex dielectric permittivity given by well-known mixing models [4], [5]. The interference pattern technique (IPT) is based on the measurement of power fluctuations of the vertical polarized signal given by the interference of the direct and reflected GNSS signals [6]–[8]. The bistatic method is based on the measurement of direct and reflected signals and the evaluation of the SNR [9], [10].

In this work, *in situ* GNSS-R campaigns in two well-known environments are described. The first experimental field is located in Grugliasco, Torino, Italy [11]. The soil is 70% sand [12], and it is covered by nonirrigated permanent meadows. The second area is located in Agliano, Asti, Italy, and it has a soil composition with 52% silt and 37% clay. The dielectric constant was evaluated from the LH reflected signal coming from satellites with a high elevation angle and the results compared with local measurements based on time-domain reflectometry (TDR).

The data collected by a GNSS receiver prototype were also analyzed. This prototype was developed by Istituto Superiore Mario Boella (ISMB) in the framework of the Italian project SMAT-F2 (System of Advanced monitoring of the Territory – phase 2). It can be easily installed on small aircraft due to its light weight and small size. During the December 11, 2014, measurements, the aircraft flew over the area around the Avigliana Lakes, Torino, Italy. Both direct and reflected GPS signals were measured using a right-hand circular-polarized (RHCP) and a left-hand circular-polarized (LHCP) antenna, respectively.

The power ratio of LHCP-reflected SNR over direct RHCP SNR was evaluated, regardless of the surface roughness and incoherent components. The reflected signal was processed with an open-loop approach, in order to obtain delay Doppler maps (DDMs) and the corresponding delay waveforms. SNRs time series were estimated from several noncoherently integrated delay waveforms. A calibration process was performed using the signals reflected from the lakes. The reflectivity obtained from different satellites was related to the type of terrain.

II. Retrieval Process from LHCP Reflected Signals

In this section, the retrieval of the dielectric constant assuming a perfectly smooth surface (specular reflection) is described (see Fig. 1). In this case, the reflected GPS signals are predominately LHCP [13], [14], especially for satellites with high elevation (angles greater than 60°).

The total electromagnetic field received by the down-looking antenna is the sum of various contributions scattered from the Earth's surface. Two kinds of contributions can be defined: coherent and incoherent. In the coherent part, the phase distribution is constant, while in the incoherent part the phase is random and uniformly distributed over an interval of 2π. In [15] it is shown

Manuscript received September 16, 2015; revised March 24, 2016 and June 01, 2016; accepted June 10, 2016. This work was supported in part by the SMAT-F2 project of Regione Piemonte.

Y. Jia and P. Savi are with the Electronic and Telecommunication Department, Politecnico di Torino, Torino 10129, Italy (e-mail: yan.jia@polito.it; patrizia.savi@polito.it).

D. Canone is with the Dipartimento Inter-ateneo di Scienze Progetto e Politiche del Territorio (DIST), Politecnico e Università di Torino, Torino 10125, Italy (e-mail: davide.canone@unito.it).

R. Notarpietro was with the Electronic and Telecommunication Department, Politecnico di Torino, Torino 10129 Italy. He is now with the EUMETSAT, Darmstadt 64295, Germany (e-mail: riccardo.notarpietro@eumetsat.int).

Color versions of one or more of the figures in this paper are available online at http://ieeexplore.ieee.org.

Digital Object Identifier 10.1109/JSTARS.2016.2584092

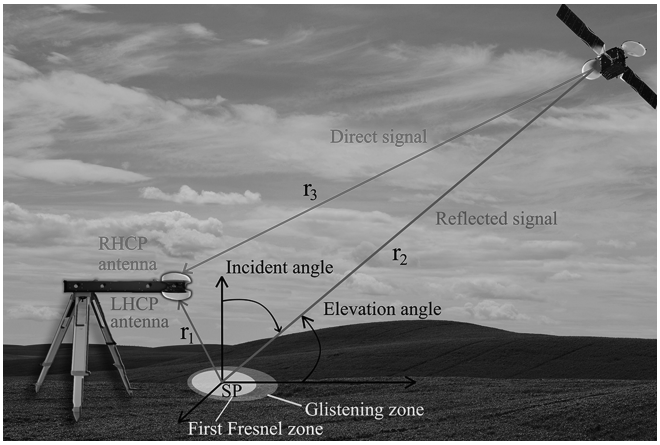

Fig. 1. Bistatic radar geometry.

that, for a smooth surface the coherent contribution is mainly LH polarized.

L-band signals are not impacted by atmospheric attenuation and normally have a good penetration through vegetation [15]. If the surface can be considered smooth, the noncoherent component assumes very low values that can be ignored and the total power received by the antenna can be approximated with the coherent part only [13].

The retrieval process aims to establish the link between received LHCP reflected signals and the dielectric constant of the soil. From the dielectric constant, if the characteristics of the soil are known, the soil moisture can be obtained by applying several well-established models (see, for example, the empirical model given in [16] and [17]). These models may be useful for the monitoring of a field of known characteristics in terms of sand, clay percentage, etc. In a general case, more powerful techniques of inverse scattering should be used.

The bistatic radar equation describes the coherent component in the GPS bistatic radar. Subscript lr represents the scattering when a satellite incident signal (RH polarized) is scattered by the surface and inverts the polarization to the LH [15]:

$$P_{\mathrm{lr}}^{\mathrm{coh}} = R_{\mathrm{lr}} \frac{P_t G_t G_r \lambda^2}{(4\pi)^2 (r_1 + r_2)^2} \tag{1}$$

where P_t is the transmitted signal power, G_t is the transmitter antenna gain, G_r is the receiver antenna gain and λ is the wavelength ($\lambda = 19.042$ cm for GPS L1 signal), r_1 is the distance between the receiver and the specular point, r_2 between the specular point and the satellite, and R_{lr} is the power reflectivity, which depends on the surface roughness as [18]

$$R_{\mathrm{lr}}(\theta) = |\Gamma_{\mathrm{lr}}(\theta)|^2 \chi(z) \tag{2}$$

where Γ_{lr} is the Fresnel reflection coefficient and $\chi(z)$ is the probability density function of the surface height z. Under the assumption of a perfectly flat surface $\chi(z) = 1$.

Combining (1) and (2), the processed SNR of peak power can be written as

$$\mathrm{SNR}_{\mathrm{peak}}^{\mathrm{refl}} = \frac{P_{\mathrm{lr}}^{\mathrm{coh}} G_D}{P_N} = \frac{P_t G_t G_r \lambda^2 G_D}{(4\pi)^2 (r_1 + r_2)^2 P_N} |\Gamma_{\mathrm{lr}}|^2 \tag{3}$$

where P_N is the noise power and G_D is the processing gain due to the de-spread of the GPS C/A code. The SNR peak power of the direct RHCP signal is

$$\mathrm{SNR}_{\mathrm{peak}}^{\mathrm{dir}} = \frac{P_t G_t G_r \lambda^2 G_D}{(4\pi)^2 {r_3}^2 P_N} \tag{4}$$

where r_3 is the distance between the transmitter and receiver. It has to be noted that the receiver gain G_r and noise power P_N of the direct signal (4) are not equal to those in (3) for the reflected signal. Therefore, a calibration process is needed. The ratio of the reflected SNR (3) over the direct SNR (4) is given by

$$\frac{\mathrm{SNR}_{\mathrm{peak}}^{\mathrm{reflect}}}{\mathrm{SNR}_{\mathrm{peak}}^{\mathrm{direct}}} = \frac{r_3^2}{(r_1 + r_2)^2} |\Gamma_{\mathrm{lr}}|^2 \, C \tag{5}$$

where C is a calibration parameter summarizing the uncertainties of G_r and P_N.

The reflection coefficient Γ_{lr} can be written as a linear combination of vertical and horizontal polarization [19]

$$\Gamma_{\mathrm{lr}} = \frac{1}{2} (\Gamma_{\mathrm{vv}} - \Gamma_{\mathrm{hh}}) \tag{6}$$

where Γ_{vv} and Γ_{hh} are the Fresnel coefficients for horizontal and vertical polarization [20]

$$\begin{aligned} \Gamma_{\mathrm{hh}}(\theta) &= \frac{\cos\theta - \sqrt{\varepsilon_r - \sin^2\theta}}{\cos\theta + \sqrt{\varepsilon_r - \sin^2\theta}} \\ \Gamma_{\mathrm{vv}}(\theta) &= \frac{\varepsilon_r \cos\theta - \sqrt{\varepsilon_r - \sin^2\theta}}{\varepsilon_r \cos\theta + \sqrt{\varepsilon_r - \sin^2\theta}} \end{aligned} \tag{7}$$

where θ is the incident angle, $\varepsilon_r = \varepsilon_{r2}/\varepsilon_{r1}$ in which ε_{r2} is the complex permittivity of the soil and ε_{r1} is the complex permittivity of the air. For the soil (dry and wet) the imaginary part of the permittivity can be neglected [21], [22]. With this hypothesis, the real part of the permittivity can be obtained from (3) together with (6), when only the LH reflected signal is known. If the LH reflected signal is normalized to the direct signal, the real permittivity can be obtained from (5) with water calibration. For satellites with high elevation angles $|\Gamma_{\mathrm{vv}}| = |\Gamma_{\mathrm{hh}}|$, the real part of the permittivity can be obtained by solving the equation for Γ_{vv} [23], or for Γ_{hh} as in [22] and [24].

III. Static Measurements

Several static measurements were carried out in two different sites. The first site is a controlled environment located in Grugliasco, Torino (45°03'58.5"N, 7°35'33.8"E), in the Dipartimento Inter-ateneo di Scienze Progetto e Politiche del Territorio (DIST). In this place, a wide field of known characteristics (mainly 50% sand) was available. The second site located in Agliano (44° 47'29.1"N, 8° 15'19.8"E) is an area of smooth hills mainly devoted to wine production. In this second case, the composition of the soil is 50% silt and 37% clay.

GNSS-R equipment and TDR setup were used to make measurements before and after rain in bare fields, which were intentionally chosen due to their different terrain composition. Data obtained with GNSS-R measurements are related to TDR

TABLE I
COMPOSITION OF THE SOIL FOR THE GRUGLIASCO EXPERIMENT

Coarse Sand(%)	Fine Sand(%)	Very Fine Sand(%)	Coarse Silt(%)	Fine Silt(%)	Clay(%)	Organic Matter(%)
15.5	50.1	16.1	5.3	8.2	4.8	1.4

TABLE II
COMPOSITION OF THE SOIL FOR THE AGLIANO EXPERIMENT

Coarse Sand(%)	Fine Sand(%)	Coarse Silt(%)	Fine Silt(%)	Clay(%)	Organic Matter(%)
1.1	10.5	6.4	44.5	36.8	0.7

Fig. 2. Static measurement setup in grugliasco (left panel) and agliano (right panel).

measurements that can provide high resolution and reliable permittivity profiles [25]. In the following, four campaigns are discussed in details:

1) Grugliasco (dry condition), January 27, 2016
2) Agliano (dry condition), February 5, 2016
3) Grugliasco (wet condition), March 3, 2016
4) Agliano (wet condition), March 7, 2016.

In Tables I and II, the composition (volume percentage and type of sand, clay) of the soil for the two sites is reported. According to the United States Department of Agriculture (USDA) Classification System, the soil of the sites of Grugliasco and Agliano belong to the loamy sand and silty clay loam textural classes, respectively [26].

The GNSS-R system consists of two commercial front-ends connected to two antennas and PCs for data acquisition. The antennas and the front ends were mounted on a metal bar fixed on a tripod for a more efficient adjustment of the orientation of the antennas (see Fig. 2). The RHCP antenna was pointing upwards for the measurement of the direct signal, while the antenna with LH circular polarization was pointing downwards for the measurement of the reflected signal [27], [28].

The antennas used in the setup were active antennas produced by ANTCOM Corp. [29] and are able to receive a GPS signal in L1 band and L2 band with LH and RH polarizations. The receivers used were SiGe GN3S v2 USB RF front-end, developed by the Colorado Center For Astrodynamics Research [30]. The acquisition of GPS data received by the antennas were performed by using N-Grab GNSS data grabber developed by the NavSAS group [31]. The raw data collected by the N-Grab were post-processed for obtaining the SNR of each satellite.

The values of the permittivity obtained from the GNSS-R signals were compared with the results obtained from local measurements based on the time-domain reflectometry (TDR) technique [32]. The measurements were performed with a three-rod sensor (length 15 cm) and Tektronix Metallic Cable Tester 1502 manufactured by Tektronix Inc., Beaverton, OR, USA. The position of the TDR sensor was not perpendicular to the terrain but tilted to 30°. In this position, only around 7 cm of the surface were taken into account in the TDR measurements. This was done in order to compare the TDR results with those obtained with GNSS-R that sense only the first few centimeters of the surface. The major axis of the Fresnel zone (the region surrounding the specular point from which power is reflected with a phase change across the surface constrained to π radians, see Fig. 1) for satellites in our geometrical condition (high elevation angle and a height of tripod of 1.5 m) was around 1 m. The TDR portable system was then moved around to cover this area. An average value of permittivity and soil moisture were obtained.

A. Measurements in Grugliasco

The static measurement setup in Grugliasco is shown in Fig. 2 (left panel). The bar on which the antennas were mounted was kept horizontal at a height of 1.45 m.

Concerning the TDR measurement, the value of permittivity was obtained for each measurement from the travel time along the TDR probe and an average value of 6.4 in dry condition was calculated. By considering the average value of 7 for the permittivity and using the model reported in [25], a soil moisture of 10% can be estimated. The soil moisture calculated from the permittivity is very low because the measurement was performed after a long period of drought. The soil moisture calculated is close to the minimum observable value in the experimental field, and is consistent with the results of [11]. After a rainy period of one week the average measured value was 9 corresponding to a soil moisture of 16%.

In Table III, the average values of SNR were obtained on January 27 (dry condition) and March 3 (wet condition). The values of permittivity were obtained from (3) with considering the Γ_{vv} component. It was observed that the values with an elevation angle greater than 60° are close to those results obtained by TDR technique. For PRN 6 and PRN24 that have low elevation angles, the approximation of $|\Gamma_{\mathrm{vv}}| = |\Gamma_{\mathrm{hh}}|$ could not be applied. Moreover, the results of PRN13 are not very good. This is probably due to some interferences caused by the position of this satellite with respect to the receiving antenna.

B. Measurements in Agliano

The same measurements were carried out in Agliano (see Fig. 2 right panel). In Table IV, the average values of SNR

TABLE III
RESULTS FOR GRUGLIASCO: DRY CONDITION AND WET CONDITION

Meas.	PRN 23			PRN 9			PRN 6		
	Ele (deg)	SNR(dB)	Eps	Ele (deg)	SNR(dB)	Eps	Ele (deg)	SNR(dB)	Eps
1 dry	77.7	5	6	63.2	3	5	50.5	−5	2
2 dry	70.9	4	6	70	3	5	55.2	1	4
	PRN15			PRN13			PRN24		
	Ele (deg)	SNR(dB)	Eps	Ele (deg)	SNR(dB)	Eps	Ele (deg)	SNR(dB)	Eps
1 wet	72	10	8	59.7	6	4	43.8	0.5	3
2 wet	72.2	11	9	58.7	4	3	44.2	−3	2

TABLE IV
RESULTS FOR AGLIANO: DRY CONDITION AND WET CONDITION

Meas.	PRN 13			PRN 28			PRN 15		
	Ele (deg)	SNR(dB)	Eps	Ele (deg)	SNR(dB)	Eps	Ele (deg)	SNR(dB)	Eps
1 dry	79.6	12	18	52.6	7	6	57.5	11	16
2 dry	73.7	13	15	63	11	14	48.1	7	10
	PRN 30			PRN7			PRN5		
	Ele (deg)	SNR(dB)	Eps	Ele (deg)	SNR(dB)	Eps	Ele (deg)	SNR(dB)	Eps
1 wet	72.5	13	24	67.8	9	20	49.1	6	11
2 wet	83	14	22	57.1	8	19	50.1	6	10

obtained on February 5 (dry condition) and March 7 (wet condition) are shown. In this case, the average relative permittivity measured by TDR in dry condition was 15. After a rainy period of one week, the average measured value was 22. These values of permittivity correspond to a soil moisture of 28% and 36%, respectively. As in the previous case, the values of permittivity obtained by the GNSS-R measurements are close to those of TDR results only for satellites with high elevation angles.

IV. ON-BOARD MEASUREMENTS

A. GNSS Receiver Prototype

A GNSS receiver prototype was developed by Istituto Superiore Mario Boella (ISMB) [33] in the framework of the Italian project SMAT-F2 (System of Advanced monitoring of the Territory – phase 2). The hardware architecture consists of two double-chain radio frequency front-ends and a microprocessor board. The front-end receivers produced by NSL Stereo [34] are connected to a microprocessor board developed based on the Open-Android (ODROID)-X2 platform [35]. The system is mounted in a carbon fiber box, specifically designed with a wing profile for aerodynamic requirements. The prototype dimensions are 75 mm $\times$ 150 mm $\times$ 250 mm and its weight is less than 3 kg making it sufficiently light and compact to be mounted on board small aircrafts or UAV. Two antennas were connected to the front-ends. One was a conventional GNSS L1 patch, up-looking RHCP antenna, to receive the direct signal from satellites. The other down-looking antenna (LH polarized antenna of Antcom [29]) measured the signals after reflection from the ground.

Fig. 3. GNSS-R prototype mounted on digisky P92 aircraft.

The raw data were stored on board in order to be post-processed [31]. Due to the large amount of memory (GB/min) required for storing the raw data, the duration of the data collection was limited. The post-processing was made with the software SOPRANO [36]. A coherent and noncoherent integration time technique was adopted during the post-processing in order to mitigate the noise. Due to the characteristics of the reflected surface, the reflected signal is much weaker than the direct one and it is not continuous in time. Hence, in order to detect the reflected signal, a channel aiding was implemented by using the direct signal information. During data processing of reflected signals, a range of expected delays was defined depending on the direct signal delays and system geometry. The reflected peak value should appear in the range of the delays. However, when this did not occur, we adjusted the noncoherent time to repeat the search.

The optimal coherent and noncoherent time interval depends on the coherence time of the scattered signal. In GPS-reflectometry applications, a coherent time of 1 ms, combined with a number of noncoherent sums in the order of 100–1000 are generally used [27], [28]. However, for the typical altitude of the flight analyzed in this work, the expected coherence time was 0.1−0.5 s.

B. Results

The GNSS receiver prototype was mounted on a Digisky P92 aircraft (see Fig. 3) and the aircraft flew over the area around the Avigliana lakes during the measurements of December 11, 2014. The vegetation was ignored since the estimation of the quantitative impact is very difficult, being a combination of incidence angle, wavelength, biomass volume, height, and loss component induced by the dielectric constant of water-containing stalks and leaves. And it is often modeled separately from the bare soil surface as a signal attenuation proportional to vegetation water content [15].

In Fig. 4, the sky-plot of GPS satellites at the 1570th second of the flight is shown.

In the first flight route (see Fig. 5), PRN4 (elevation 78°) and PRN32 (elevation 87°) were considered because the specular points corresponding to these satellites fell on the lakes' surfaces and it was possible to calibrate the system.

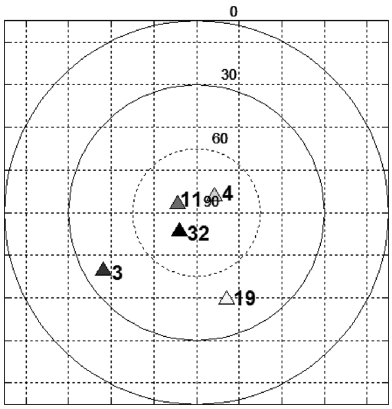

Fig. 4. Skyplot December 11 flights.

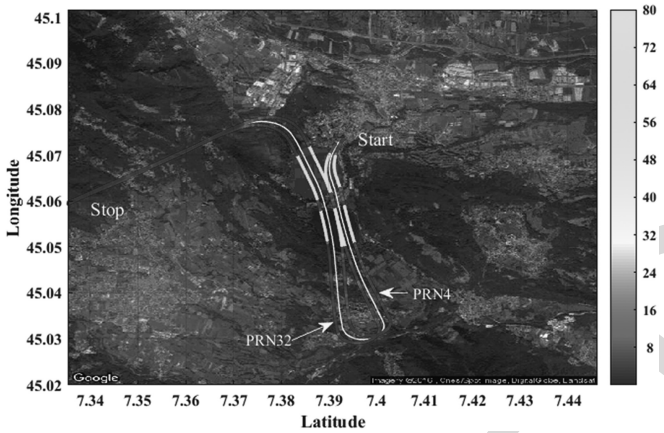

Fig. 5. Route flight (yellow line), specular reflection points of PRN4 and PRN32 with the levels of dielectric constant values.

The reflected signals were postprocessed with an open-loop approach, in order to obtain delay Doppler maps (DDMs) and the corresponding delay waveforms. SNRs time series were estimated from noncoherently integrated delay waveforms. Both direct and reflected signals were processed to obtain the SNR and a calibration process was performed through the over-water condition to determine the calibration constant C of (5).

In Figs. 6 and 7, the normalized power reflectivity of LH reflected signal normalized to RH direct signal are shown. The high reflectivity values correspond to the return flight over the two lakes. The values of the real part of permittivity were obtained from (5) and (6). They are superimposed on google map as shown in Fig. 5. On the lakes, the value of permittivity is around 80, whereas on the land is from 4 to 30.

In the second flight route (see Fig. 8), PRN 3 (elevation 38.2°), 11 (elevation 80.3°), and 19 (elevation 46.7°) are also taken into account. In this case only the PRN11 has a great elevation angle. The reflection points for these satellites are also shown in Fig. 8. The normalized reflectivity is shown in Fig. 9. High values of reflectivity correspond to the presence of the almost specular reflecting surface of the lake. This is confirmed also for low elevation satellites such as PRN19 and PRN3.

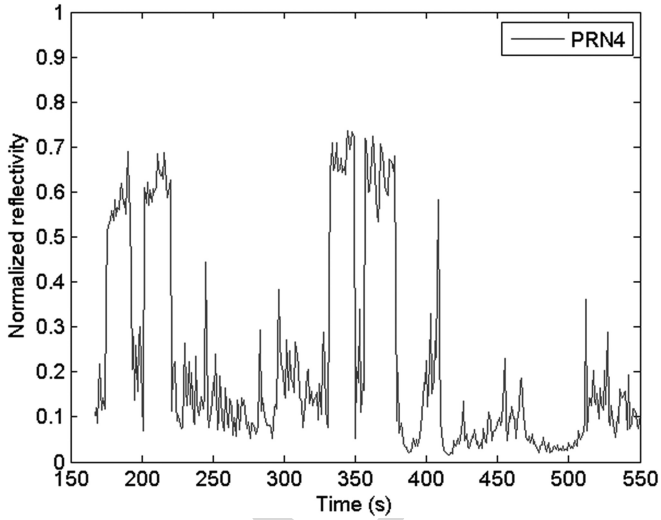

Fig. 6. Normalized power reflectivity of PRN4.

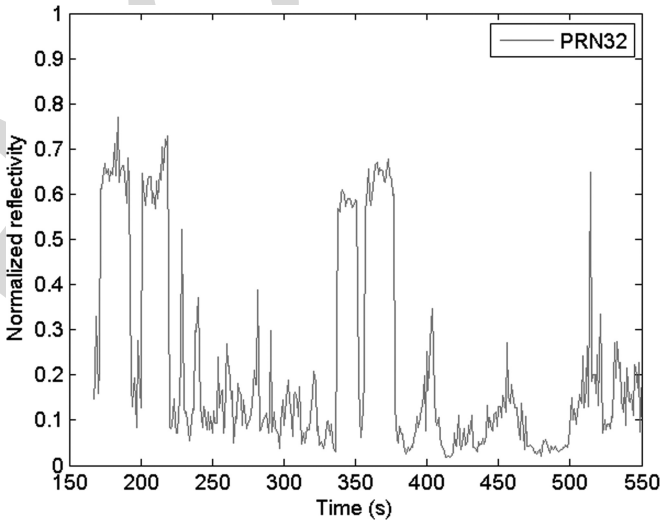

Fig. 7. Normalized power reflectivity of PRN32.

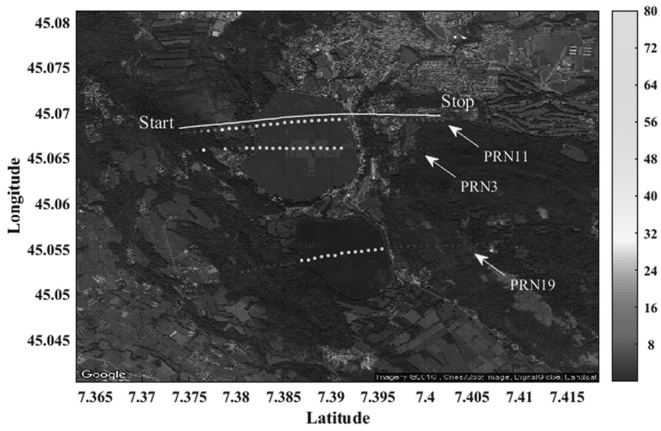

Fig. 8. Route flight (yellow line), specular reflection points of PRN3, PRN11, and PRN19 with the levels of dielectric constant values.

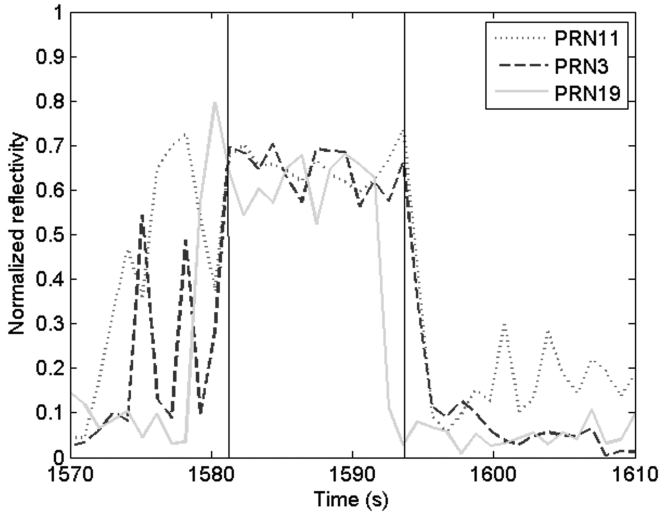

Fig. 9. Normalized power reflectivity of PRN11, PRN3, and PRN19.

In Fig. 8, the values of the real part of the permittivity are also shown and are in good agreement with the land and water condition.

V. Conclusion

The use of GNSS-R reflected signals to monitor the Earth's surface was analyzed with *in situ* and on-board measurements. The values of the dielectric constant obtained with *in situ* GNSS-R measurements were compared with TDR results for validating the retrieval process. Data collected during a flight over the Avigliana lakes by a GNSS receiver prototype developed by the Istituto Superiore Mario Boella (ISMB) were post-processed with an open-loop approach, Delay Doppler Maps and delay waveforms were obtained. The power reflectivity evaluated as the ratio of LH reflected signal to the direct RH signal and the estimated real permittivity showed good correlation with the types of underlying terrain.

Acknowledgment

The authors would like to thank the Istituto Superiore Mario Boella (ISMB) for the realization of the prototype, Digisky s.r.l. (Turin, Italy) for the flight campaigns performed with the Tecnam P92 aicraft and the Istituto per le Piante da Legno e Ambiente - I.P.L.A. S.p.A. for the individuation of the site for the static campaign.

References

[1] S. Jin, E. Cardellach, and F. Xie, *GNSS Remote Sensing: Theory, Methods and Applications*. New York NY, U.S.A.: Springer, 2014.

[2] C. Li, W. Huang, and S. Gleason, "Dual antenna-space based GNSS-R ocean surface mapping: Oil slick and tropycal cyclone sensing," *IEEE J. Sel. Top. Appl. Earth Obs. Remote Sens.*, vol. 8, no. 1, pp. 425–435, Jan. 2015.

[3] A. Alonso-Arroyo, A. Camps, H. Park, D. Pasqual, R. Onrubia, and F. Martin, "Retrieval of significant wave height and mean sea surface level using the GNSS-R interference pattern technique: Results from a three-month field campaign," *IEEE Trans. Geosci. Remote Sens.*, vol. 53, no. 6, pp. 3198–3209, Jun. 2015.

[4] V. U. Zavorotny, K. M. Larson, J. J. Braun, E. E. Small, E. D. Gutmann, and A. L. Bilich, "A physical model for GPS multipath caused by land reflections: Towards bare soil moisture retrieval," *IEEE J. Sel. Top. Appl. Earth Obs. Remote Sens.*, vol. 3, no. , pp. 100–110, Mar. 2010.

[5] K. M. Larson, J. J. Braun, E. E. Small, V. U. Zavorotny, E. D. Gutmann, and A. L. Bilich, "GPS multipath and its relation to near- surface soil moisture content," *IEEE J. Sel. Top. Appl. Earth Obs. Remote Sens.*, vol. 3, no. 1, pp. 91–99, Mar. 2010.

[6] N. Rodriguez-Alvarez, X. Bosch-Luis, A. Camps, *et al.*, "Soil moisture retrieval using GNSS-R techniques: Experimental results over a bare soil field," *IEEE Trans. Geosci. Remote Sens.*, vol. 47, no. 11, pp. 3616–3624, Nov. 2009.

[7] V. L. Mironov, S. V. Fomin, V. M. Konstantin, V. S. Anatoliy, and M. I. Mikhaylov, "The use of navigation satellites signals for determination the characteristics of the soil and forest canopy," in *Proc. IEEE Int. Symp. Geoscie. Remote Sens., Munich*, Germany, 2012, pp. 7527–7529.

[8] V. L. Mironov and K. V. Muzalevskiy, "The new algorithm for retrieval of soil moisture and surface roughness from GNSS reflectometry," *IEEE Int. Symp. Geosci. Remote Sens. Symp., Munich*, Germany, 2012, pp. 7530–7532.

[9] S. Katzberg, O. Torres, M. Grant, and D. Masters, "Utilizing calibrated GPS reflected signals to estimate soil reflectivity and dielectric constant: Results from SMEX02," *Remote Sens. Environ.*, pp. 17–28, 2005.

[10] A. Egido, M. Caparrini, G. Ruffini, S. Paloscia, E. Santi, L. Guerriero, N. Pierdicca, and N. Floury, "Global navigation satellite systems reflectometry as a remote sensing tool for agriculture," *Remote Sens.*, vol. 4, no. 8, pp. 2356–2372, 2012.

[11] M. Baudena, I. Bevilacqua, D. Canone, S. Ferraris, M. Previati, and A. Provenzale, "Soil water dynamics at a midlatitude test site: Field measurements and box modeling approaches," *J. Hydrol.*, vol. 414–415, pp. 329–340, 2012. [Online]. Available: http://dx.doi.org/10.1016/j.jhydrol.2011.11.009

[12] D. Canone, S. Ferraris, G. Sander, and R. Haverkamp, "Interpretation of water retention field measurements in relation to hysteresis phenomena," *Water Resour. Res.*, vol. 44, no. 4, pp. 1–14, 2008, W00D12. [Online]. Available: http://dx.doi.org/10.1029/2008WR007068

[13] D. Masters, A. Penina, and S. Katzberg, "Initial results of land-reflected GPS bistatic radar measurements in SMEX02," *Remote Sens. Environ.*, vol. 92, no. 4, pp. 507–520, 2004.

[14] F. Martín, F. M. Juan, A. Albert, V. l. Mercedes, C. Jordi, C. Adriano, M. Piles, L. Pipia, A. Tardà, and G. V. Alberto, "Airborne soil moisture determination using a data fusion approach at regional level," in *Proc. IEEE Int. Symp. Geosci. Remote Sens. Symp.*, 2011, pp. 3109–3112.

[15] R. D. De Roo and F. T. Ulaby, "Bistatic specular scattering from rough dielectric surfaces," *IEEE Trans. Antennas Propag.*, vol. 42, no. 2, pp. 220–231, Feb. 1994.

[16] M. C. Dobson, F. T. Ulaby, M. T. Hallikainen, and M. A. El-Rayes, "Microwave dielectric behaviour of wet soil—Part I: Empirical models and experimental observation," *IEEE Trans. Geoscie. Remote Sens.*, vol. 23, no. 1, pp. 25–34, Jan. 1985.

[17] J. Wang and T. Schmugge, "An empirical model for the complex dielectric permittivity of soils as a function of water content," *IEEE Trans. Geoscie. Remote Sens.,* vol. GE-18, no. 4, pp. 288–295, Oct. 1980.

[18] P. Beckmann and A. Spizzichino, *The Scattering of Electromagnetic Waves from Rough Surfaces*. Norwood, MA, USA: Artech House, 1963.

[19] W. L. Stutzman, *Polarization in Electromagnetic Systems*. Boston, USA: Artech House, 1993.

[20] R. Janaswamy, *Radiowave Propagation and Smart Antennas for Wireless Communications*. Norwell, MA, USA: Kluwer, 2001.

[21] J. Behari, Microwave Dielectric Behaviour of Wet Soils. Springer Science & Business Media. New York, USA., 2006.

[22] S. Hong and I. Shin, "A physically-based inversion algorithm for retrieving soil moisture in passive microwave remote sensing," *J. Hydrol.*, vol. 405, no. 1, pp. 24–30, 2011.

[23] A. Egido, G. Ruffini, M. Caparrini, C. Martín, E. Farrés, and X. Banqué, "Soil moisture monitorization using GNSS reflected signals," in *Proc. First Colloq. Sci. Fundam. Aspects Galileo Programme, Toulouse, France*, 2007, pp. 1–4.

[24] T. J. Jackson, R. Hurkmans, A. Hsu, and M. H. Cosh, "Soil moisture algorithm validation using data from the Advanced Microwave Scanning Radiometer (AMSR-E) in Mongolia," *Italian J. Remote Sens.*, vol. 30/31, pp. 39–52, 2004.

[25] G. C. Topp, J. L. Davis, and A. P. Annan, "Electromagnetic determination of soil water content: Measurements in coaxial transmission lines," *Water Resour. Res.*, vol. 16, no. 3, pp. 574–582, 1980.

[26] Soil Survey Laboratory Staff, "*Soil survey laboratory methods manual." USDA-SCS U.S. Government Printing Office*, Washington, DC, USA, *Soil Survey Investigations Report no. 42, Version 2.0.,* 1992.
[27] Y. Pei, R. Notarpietro, P. Savi, and M. Pini, "A fully software GNSS-R receiver for soil dielectric constant monitoring," 15th *Int. Conf. Electromagnet. Advanc. App. (ICEAA13)*, Torino, Italy, Sep. 9–13, 2013..
[28] Y. Pei, R. Notarpietro, P. Savi, and F. Dovis, "A fully software GNSS-R receiver for soil monitoring," *Int. J. Remote Sens.*, vol. 35, no. 6, pp. 2378–2391, 2014.
[29] Dual Polarization ANTCOM Antennas Catalog. Antcom Corp., Torrance, CA, USA. [Online] http://www.antcom.com/documents/catalogs/RHCP-LHCP-V-H-L1L2GPSAntennas.pdf (accessed on 30 June 2016).
[30] Colorado Center for Astrodynamics Research. Denver, CO, USA. [Online]. http://ccar.colorado.edu/gnss/ (accessed on 30 June 2016).
[31] Navigation Satellite System Group, Politecnico di Torino, Torino, TO, Italy. [Online]. http://www.det.polito.it/research/research_areas/telecommunications/navsas(accessed on 30 June 2016).
[32] P. Savi, I. A. Maio, and S. Ferraris, "The role of probe attenuation in the time-domain characterization of dielectrics," *Electromagnetics*, vol. 30, no. 6, pp. 554–564.
[33] Istituto Superiore Mario Boella (ISMB), Torino, Italy. [Online]. Available: http://www.ismb.it/
[34] NSL Stereo FE. [Online]. Available: http://www.nsl.eu.com/primo.html, accessed June 6, 2015.
[35] ODROID-X2 Platform. [Online]. Available: http://www.hardkernel.com/main/products/, accessed June 6, 2015.
[36] E. Falletti, D. Margaria, M. Nicola, G. Povero, and M. T. Gamba, "N-FUELS and SOPRANO: Educational tools for simulation, analysis and processing of satellite navigation signals," presented at the *IEEE Int. Conf. Frontiers Educ.*, Oklahoma City, USA, Oct. 23–26, 2013.

Yan Jia received the M.S. degree in telecommunications engineering from Politecnico di Torino, Turin, Italy, in 2013, where she is currently working toward the Ph.D. degree in electronics engineering.

Since 2013, she has been working in the Department of Electronics and Telecommunications, Politecnico di Torino, where she was involved in the GNSS-R antenna analysis. In 2014, she worked in the SMAT project, mainly focusing on the retrieval of soil moisture and biomass content. Her current research interests include Global Navigation Satellite System Reflectometry (GNSS-R) applications to land remote sensing and antenna design.

Patrizia Savi (SM'16) received the Laurea degree in electronic engineering from the Politecnico di Torino, Turin, Italy in 1985.

In 1986, she was a consultant in Alenia (Caselle Torinese, Italy) where she conducted research on the analysis and design of dielectric radomes. From 1987 to 1998, she was a Researcher with the Italian National Research Council. In 1998, she joined the Dipartimento di Elettronica, Politecnico di Torino, as an Associate Professor, where she is currently involved in teaching a course on electromagnetic field theory. Her current research interests include dielectric radomes, frequency-selective surfaces, waveguide discontinuities and microwave filters, high-altitude platform (HAP) propagation channels, Global Navigation Satellite System Reflectometry (GNSS-R) for soil moisture retrieval, microwave analysis, and characterization of carbon fiber and carbon nanotubes.

Davide Canone received the Graduate degree in forest and environmental sciences at the Agronomy Faculty of the University of Turin, Turin, Italy, in 2004, and the Ph.D. degree in agricultural, forest, and food sciences, curriculum agro-forest and agro-industrial economy and engineering from the University of Turin.

He collaborated with the Department of Agricultural, Forest, and Environmental Economics and Engineering (DEIAFA)—Division of Agricultural Hydraulics, University of Turin, from the year 2005. During the year 2007, he stayed six months at the Laboratory of Soil and Environmental Physics of the Federal Polytechnic of Lausanne, Switzerland, where he was involved in working on the characteristics of acoustic emissions during fluid front displacement in porous media. In August 2007, he was an Assistant Professor at the University of Turin. He is currently an Assistant Professor at the Interuniversity Department of Urban and Regional Studies and Planning of the Polytechnic and the University of Turin.

Riccardo Notarpietro received the Telecommun. Eng. Degree and the Ph.D. degree from Politecnico di Torino, Torino, Italy, in 1998 and in 2001, respectively, with a thesis on the subject of the atmosphere remote sensing exploiting GPS measurements from space and from ground.

He was an Assistant Professor in Electromagnetic Fields at Politecnico di Torino from 2006 to 2014. He was member of the Remote Sensing Group operating inside the Electronics Department. His main research areas were related to the retrieval of atmospheric profiles from GNSS Radio Occultation observations but also to the monitoring of soil properties using GNSS Reflectometry and to the tomographic reconstruction of 3-D water vapor fields using GNSS ground-based measurements. His fields of activities included also electromagnetic wave propagation and radarmeteorology. Since 2014 he is with EUMETSAT, Darmstadt, Germany, and providing support for the development of the new radio occultation mission on board the future European Polar System-Second Generation satellites.